Society For Biomaterials

Structural analysis of fluorine-containing bioactive glass nanoparticles synthesized by sol–gel route assisted by ultrasound energy

Carolina E. C. Lins,[1] Agda A. R. Oliveira,[1,2] Ismael Gonzalez,[3] Waldemar A. A. Macedo,[3] Marivalda M. Pereira[1]

[1]Departamento de Engenharia Metalúrgica e de Materiais, Universidade Federal de Minas Gerais, Belo Horizonte, Brazil
[2]Department of Research and development, JHS Biomateriais, Sabará, Brazil
[3]Department of Applied Physics, Centro de Desenvolvimento da Tecnologia Nuclear, CDTN, Belo Horizonte, MG, Brazil

Received 22 June 2016; revised 12 December 2016; accepted 19 December 2016
Published online 2 February 2017 in Wiley Online Library (wileyonlinelibrary.com). DOI: 10.1002/jbm.b.33846

Abstract: In the last decades, studies about the specific effects of bioactive glass on remineralization of dentin were the focus of attention, due to their excellent regenerative properties in mineralized tissues. The incorporation of Fluorine in bioactive glass nanoparticles may result in the formation of fluorapatite (FAP), which is chemically more stable than hydroxyapatite or carbonated hydroxyapatite, and therefore is of interest for dental applications. The aim of this study was to synthesize and characterize a new system of Fluorine-containing bioactive glass nanoparticles (BGNPF). A sol-gel route assisted by ultrasound was used for the synthesis of BGNPF. The particles obtained were characterized by scanning electron microscopy (SEM), energy dispersive spectroscopy (EDS), atomic force microscopy (AFM), X-ray diffraction (XRD), dynamic light scattering (DLS), nitrogen adsorption, and X-ray photoelectron spectroscopy (XPS). SEM micrographs showed that the particles are quite uniform spherical nanostructures, occurring agglomeration or partial sinterization of the particulate system after heat treatment. XRD and XPS analysis results suggest the formation of fluorapatite crystals embedded within the matrix of the bioactive glass nanoparticles. © 2017 Wiley Periodicals, Inc. J Biomed Mater Res Part B: Appl Biomater, 106B: 360–366, 2018.

Key Words: biomaterial, material design, nanoparticle, bioactive glass, fluorine-containing

How to cite this article: Lins CEC, Oliveira AAR, Gonzalez I, Macedo WAA, Pereira MM. 2018. Structural analysis of fluorine-containing bioactive glass nanoparticles synthesized by sol–gel route assisted by ultrasound energy. J Biomed Mater Res Part B 2018:106B:360–366.

INTRODUCTION

The improvement in oral health has brought benefits to the population, causing the teeth to be kept longer in the oral cavity. However, at the same time, it has increased the incidence of other problems such as dentinal hypersensitivity (HD). With the decline of caries and periodontal disease, the treatment of dentin hypersensitivity is gaining priority.[1] Dentin hypersensitivity is characterized by localized, acute, non-spontaneous pain, and occurs in response to some stimulus. This pain is caused by loss of the tooth structure, which results in exposure of dentinal tubules to the oral environment. Various methods for the treatment of dentinal hypersensitivity were investigated; however, none is completely effective.

For some patients, the dentinal hypersensitivity may present only a minor inconvenience, but for many the degree of discomfort and emotional distress can be very detrimental. With increasing life expectancy, gingival recession and erosion problems tend to increase. In addition, the discomfort caused by dentin sensitivity can lead to behavioral changes, such as a change in diet and inadequate plaque control, which would further increase the HD. This can also lead to tooth decay, gum inflammation and periodontal destruction.[1–3]

Several therapeutics have been proposed for the treatment of dentin hypersensitivity, and their modes of action are based on blocking neural activation and transmission of pain stimuli, through the use of desensitizing agents, and/or preventing the movement of fluid within the dentinal tubules through its occlusion.[1,3,4] Dentin hypersensitivity is considered a challenge for dental professionals due to its difficult treatment. Despite the vast literature on the subject, there is still not a final and general solution for the problem.

One of the new approaches to the more effective treatment of dentine hypersensitivity is based on the use of the properties of bioactive glass (BG), which produces a specific biological response on its surface when in contact with living tissue. Because the dental constitution is very similar to that of bone tissue, the use of BG with the ability to deposit inside the dentinal tubules was proposed, so that in the presence of oral fluids it induces the hydroxyapatite (HA) formation process, leading to a chemical bond with the material, and resulting in the occlusion of the dentinal tubules.[4,5]

In recent decades, the specific effect of bioactive glass on remineralization has been widely studied, due to its

Correspondence to: C.E.C. Lins, e-mail:inhalins@yahoo.com.br
Contract grant sponsor: CNPq, CAPES, FAPEMIG/Brazil

excellent regenerative properties in mineralized tissues. It is also known that the effect of bioactive glass can be enhanced when the material is at the nanoscale. Furthermore, the incorporation of fluorine in the materials composition can result in the formation of fluorapatite (FAP), which is chemically more stable than hydroxyapatite (HA) or carbonated hydroxyapatite (HAC) and therefore is of interest for dental applications.

A drawback to the use of bioactive glass in the particulate form incorporated into oral hygiene products—especially those where the use involves brushing or friction—is the cutting power of glass particles due to their extremely irregular, jagged and sharp edges. Thus, ground glass particles can cause microcuts on the gums, causing her irritation and possibly increasing soreness in patients. This side effect can be minimized or even eliminated if spherical particles are used. The sol–gel method used in this work has therefore as an additional advantage the possibility of obtaining spherical nanoparticles. To maintain the stability of the nanoparticles, some studies focus on obtaining spherical bioactive glass particles, to create a bioactive material with dispersion ability.[6] In this study, we used polyethylene glycol (PEG), a surfactant, to improve the dispersion of nanoparticles and/or to control its shape. Moreover, the sol–gel process has been associated with high-intensity ultrasound technique to allow the formation of bioactive glass nanoparticles with excellent capability of dispersion and bioactivity.

Bioactive glasses with a nominal composition of 60% SiO_2, 36% CaO and 4% P_2O_5 (wt %) have excellent potential for bone tissue engineering applications by presenting a high level of bioactivity and developing an HA layer.[7] Thus, in the study nanoparticles with this tri-component nominal composition were synthesized by the sol–gel route, however, adding fluorine for the development of a material with additional interest for the dental field. Brauer[8] reported the synthesis of bioactive glass containing fluorine by conventional fusion, a process that requires high temperature. In contrast, the sol-gel technology is a low-temperature preparation method and the glasses prepared by this method have a mesoporous structure with a high specific surface area.

The bioactive glasses containing fluorine synthesized by fusion[8,9] were based on the SiO_2-Na_2O-CaO-P_2O_5 system, with increasing amounts of CaF_2, maintaining the network connectivity and the proportion of all other components constant. It was also evaluated the SiO_2-CaO-P_2O_5 system with 9% fluorine. The formation of apatite on the glass powder, upon immersion in simulated body fluid at 37°C, was evaluated for 2 weeks. The results show that fluorine incorporation has resulted in the formation of FAP in the glass structure, which is chemically more stable than HA or HAC and therefore it is of interest for dental applications. However, increasing the fluorine content in the glass favored the formation of calcium fluoride (CaF_2) at the expense of FAP. The authors reported that small additions of fluorine (4.75%/mol) could affect the formation of apatite in PBS. However, it was observed that in 1 week, all glasses with a concentration above 4.75%/mol clearly showed the presence of apatite by XRD. However, by increasing the fluorine content the fluoride (CaF_2) peaks dominated the XRD pattern while the relative amount of apatite decreased. This can be explained by the fact that the glasses had low phosphate concentrations (1.07 mol% or less), which favors the formation of CaF_2 instead of apatite, since in this case there is an excess of calcium and fluoride ions, and not enough phosphate ions.[8]

Brauer and coworkers[8–10] also noted that the fluoride release did not increase with increasing fluorine content in the glass, since the fluoride concentration in PBS was greater for the glass with 9.28% CaF_2 added during synthesis than for the glass with 4.75% CaF_2 added, and decreased for concentrations above 9.28% CaF_2. This result can be explained by reprecipitation of CaF_2, which has low solubility in water, decreasing the release of fluoride, in spite of a higher concentration of fluorine in the glass. Considering the results described above, in this study, a fixed concentration of 9.28% CaF_2 was used to produce the nanoparticles.

An important factor for the synthesis of bioactive glass is the network connectivity, a measure of the number of oxygen atoms per network forming element, an indicator of solubility, reactivity and bioactivity of bioactive glass.[11] Lusvardi[12] showed in his work that network connectivity values above 2.4 describe a highly polymerized glass with a network that does not easily degrade in an aqueous medium, to a step essential to allow the formation of hydroxyapatite or fluorapatite when in contact with body fluids.

According to Brauer[8] it is very important to have an understanding of glass structure to design a new bioactive glass. As Phosphorous is present as orthophosphate, and balanced by modifier cations (Ca^{2+}, Na^{+}), when increasing the phosphate content it is necessary to raise the content of modifiers proportionally. If additional modifier cations are not provided, the orthophosphate phase will remove modifier cations from the silicate phase, resulting in an increase in network connectivity and silicate phase polymerization, and in a drastic decrease in bioactivity.

In this study, it was evaluated the preparation of bioactive glass nanoparticles containing fluorine (BGNPF) using a sol-gel route, a co-precipitation method, by controlling the concentration of reactants, catalyst, alcohol, and pH. A network connectivity of 2.13 and a composition similar to that used by Brauer[8] was used.

MATERIALS AND METHODS

The reagents used were: deionized water; 98% tetraethyl orthosilicate (TEOS), 99% triethyl phosphate (TEP) and 6000 g mol^{-1} polyethylene glycol (PEG), by Sigma–Aldrich, USA; 65% nitric acid solutions (HNO_3) and 33% ammonium hydroxide solution (NH_4OH) by Merck, USA; methanol, tetrahydrate calcium nitrate ($Ca(NO_3)_2.4H_2O$), calcium fluoride (CaF_2) and 4.2.1, hydroxy methyl cellulose (HMC) by Synth, Brazil. The solution that mimics the body fluid (SBF) was prepared according to ISO/FDIS 23317: 2007 (E).

The BGNPF was produced by the sol–gel route, according the following steps [4]: (1) 4.17 mL of TEOS and 0.14 mL of a TEP were mixed in a 10 mL of methanol–

water solution (1:2 molar ratio) with pH 1–2, adjusted with HNO_3 solution, and mixed for 10 min. (2) The sol was added dropwise in a 600 mL of 2% PEG solution with pH 12, adjusted with NH_4OH solution, and ultrasound stirred for 30 min. (3) After the reaction time, the pH of the formed sol was adjusted to 4, with HNO_3 solution and, then, (4) 4.30 g of $Ca(NO_3)_2.4H_2O$ and 0.31 g of CaF_2 were dissolved in the sol and (5) ultrasound stirred for additional 30 minutes. (6) The particles formed were separated by subsequent filtrations in 0.22 and 0.11 μm Millipore. (7) The sol filtered under 0.11 μm was freeze drying. (8) The powders obtained were thermally treated, with heating rate of 1°C min^{-1}, at 700°C for 360 min.

Bioactive glass microparticles containing 9.28% CaF_2 (BGMPF) were also synthesized for comparison with nanoparticles. TEP and TEOS were hydrolyzed in nitric acid solution (pH 1–2) for 1 h. $Ca(NO_3)_2.4H_2O$ and (CaF_2) were added to the mixture and solubilized with and without application of high-intensity ultrasound. The nominal composition of the microparticles produced was SiO_2 60%, CaO 26.72%, P_2O_5 4%, CaF_2—9.28% in weight. The resulting sol was placed in Teflon containers, kept at ambient temperature for gelation, was aged at 60°C for 72 h, and dried at increasing temperatures up to 120°C. The solid obtained was ground, sieved and the fraction with particle size bellow 38 μm was separated and heat-treated at 700°C for 180 min. The temperature 700°C was selected to allow the incorporation of Calcium and Fluorine into the glass network.

Considering the results by other authors in the literature,[9] the concentration of 9.28% calcium fluoride and network connectivity 2.13 were selected. The nominal composition of the glass synthesized in this work was (in %molar): 44.88% SiO_2, 0.97% P_2O_5, 44.87% CaO, and 9.28%CaF_2.

To obtain bioactive glass nanoparticles with excellent dispersibility and bioactivity, the sol–gel process can be simultaneously associated with high-intensity ultrasound technique. Ultrasonic cavitation (the formation, growth and collapsing of gas-filled cavities in a liquid) is responsible for the unique properties of materials made with high-intensity ultrasound. In the presence of ultrasound, the bubbles expand in touch with the sound field. During the rarefaction phase, volatile species in the surrounding bubble diffuse into the bubble to compensate the increase in volume and decrease in pressure. Chemical reactions can be conducted into the bubble, resulting in the synthesis of nanostructured materials.

The morphology of BGNPF was observed by scanning electron microscopy (SEM), using the Tecnai G220 FEI equipment, equipped with energy dispersive spectroscopy (EDS). Qualitative elemental analysis of the nanoparticles was performed by EDS analysis. The presence of fluoride was identified by XPS, as described below.

The Atomic force microscopy (AFM) analysis was performed to obtain a topographic image of the sample. This study used the AFM equipment—Park Systems XE-model-70, leading type Si PPP-NCHR, in noncontact mode, with a constant force of 42N/m and 330 kHz frequency. Sample preparation was performed by adding the powder of NPVBF after lyophilization and heat-treatment in ethanol, at the concentration of 1 mg mL^{-1}, kept stirring for 5 h, and immediately after a droplet was dispensed on a coverslip for examination.

The X-ray diffraction analysis (XRD) was performed to evaluate structural characteristics of NPVBF. XRD patterns were collected on a Philips PW1700 Series automated powder diffractometer using Cu Kα radiation ($\lambda = 1.5418$ Å) at 40 kV/40 mA. Data were collected between 4.05 and 89.951 at a step size of 0.061 and a time of 1.5 s/step.

The dynamic light scattering analysis (DLS) was performed to measure the hydrodynamic diameter of the nanoparticles in suspension prior to lyophilization. The equipment used was a Zetasizer 3000 HS 1256. This system is equipped with a 4 mW He:Ne laser at 633 nm wavelength and measures the particle size at a detection angle of 173°. Light scattering measurements were made at 25°C ± 1°C. Hydrodynamic measurements were performed at a 90° angle, after the dilution of the sample to 10 μg mL^{-1} in NaCl solution, according to ISO standards 14488:2007 and ISO 13321 Part 8:1996. The data were analyzed according to the cumulative method to determine the apparent mean diameter and polydispersity index (PDI); the final value was a mean of 10 measurements.

The isotherms of N_2 adsorption–desorption were measured at 77K in a Quantachrome9 equipment. The specific surface area was determined using the Brunauer-Emmett-Teller method (BET) method using adsorption data points at relative pressure (P/Po) in the range of 0.01–0.30. The distribution of pore diameter calculated by the BJH method was applied to the desorption curves.

X-ray photoelectron spectroscopy (XPS) measurements were performed in a surface analysis system (SPECS, Germany) equipped with a Phoibos 150 electron analyzer. Monochromatized Aluminum radiation (1486.6 eV) with an output power set at 400 W was used for all samples analysis. The C1s signal (284.6 eV) was employed as reference to calibrate the binding energies (BE) of different elements in order to correct the charge effect. CasaXPS software was used to analyze all XPS data. Surface atomic concentrations in the samples were estimated using the instrument sensitivity factors to scale for the calculated photoelectron peak areas

RESULTS AND DISCUSSIONS

Figure 1 shows a SEM micrograph of the particles obtained after freeze-drying and heat treatment and the elemental composition obtained by EDS analysis over the field shown. The qualitative assessment of the average diameter and shape of the particles suggests that the proposed method resulted in the formation of spherical particles on the nanometer scale. However, it is not possible to determine, by analyzing only the image, the actual size of the particles. In addition to Ca and Si, EDS analysis also indicated the presence of fluorine in the system.

The particle size distribution obtained by DLS analysis for BGNPF suspension before lyophilization and heat treatment

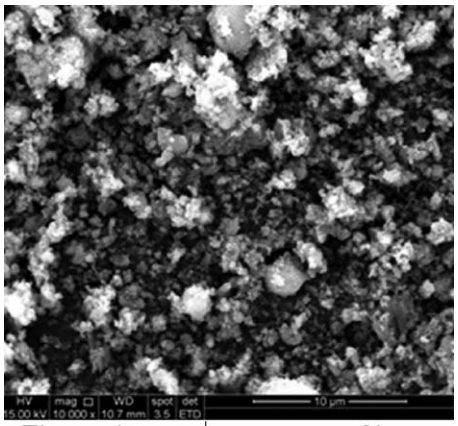

Element	%
F	23.5
Ca	26.3
Si	50.2

FIGURE 1. SEM micrograph and elemental composition obtained by EDS for BGNPF produced.

is illustrated in Figure 2. The cumulative analysis shows an average particle diameter of 5.3 ± 0.3 nm and a low polydispersity index (PDI) of 0.15 ± 0.02, which indicates a homogeneous distribution of particle size.

Morphology of the synthetized BGNPFs was also observed by AFM, as illustrated in Figure 3. It can be observed that the particles are uniform, with quite a spherical nanostructure, and the image suggests that an agglomeration or partial sinterization of the particulate system occurred after heat treatment.

Comparing the results of the particle size obtained by DLS (5.3 ± 0.3 nm) and by AFM (between 45 55 nm), is possible to observe a significant increase in the particle diameter size after the heat treatment. This fact probably is due to the large surface area of the nanoparticles, which leads to a large driving force, enough to produce growth by coalescence or another mechanism. In addition, AFM images also showed that the nanoparticles system apparently aggregated after

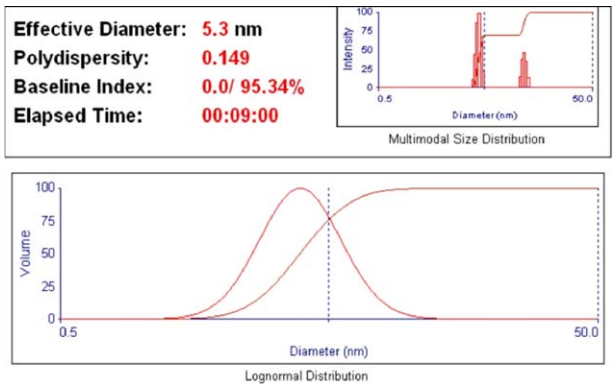

FIGURE 2. Particle size distribution of BGNPF produced, measured by DLS analysis.

heat treatment. Partial sintering may have occurred with increasing temperature.

Fine particles, primarily in the nanometer range, have large surface areas and often agglomerate to form secondary particles, to minimize the total surface or interfacial energy of the system. The agglomeration refers to the adhesion of particles that occur due to the forces of Van der Waals type, which are significantly higher in nanoparticles. Typically, an agglomerated mass can be agglomerated by means of a dispersion in a liquid medium. Because aggregation refers to particles that incipiently sintered, it is difficult to break the aggregated mass of primary particles[13]. Therefore, it is suggested that the BGNPF showed agglomeration after freeze-drying, but may have partially sintered after heat treatment.

To minimize secondary aggregation, lyophilization was used to remove water from the interface material, and the heat treatment was conducted at reduced time. However, additional studies are needed to determine the appropriate conditions of synthesis and heat treatment, to minimize the process of agglomeration and/or aggregation of the nanoparticles system produced.

It was observed (Figure 3) that the particles presented an approximate diameter of 50 nm. This result is important for the proposed application because the diameter of dentinal tubules ranges from 2–3 μm (near pulp) to 0.5–0.9 μm (near amelo-dentin junction).[1,3] Thus, reduced particle size favors the deposition thereof within the tubules, which can optimize the results of dentin hypersensitivity treatment. The main action mechanism of bioactive glass is the release of calcium and phosphate to result in supersaturation of surrounding fluids, and subsequently precipitation of HAC crystals, contributing to an increase in remineralization processes. However, it is suggested that when using nanoparticles this process occurs directly in the interior of the tubules, which may provide a more effective obstruction of the tubules, in higher thickness and depth, rather than the processes that only occur at the opening surface of the tubules. Moreover, the release of fluoride from the glass, may lead to the formation of a FAP phase, which is more stable in the acidic conditions of the oral cavity than HAC.[8–10,14] Therefore, NPVBF evaluated in this study have the potential to provide a more durable and sustained action for the treatment of HD.

Another important feature that can be observed in Figure 3 is the spherical shape shown by BGNPF. A drawback for the use of bioactive glasses in the particulate form incorporated into oral hygiene products—especially those in which the use involves brushing or rubbing—is the cutting power of glass particles due to their extremely irregular, jagged and sharp edges. This feature of glass particles is a result of multiple fractures of the material during the grinding process to produce powders with the desired particle size. Thus, the glass particles may cause microcuts in the gums, causing irritation and possibly increasing pain sensation in patients (Tirapelli et al., 2007). Considering these issues, obtaining spherical shape particles at the nanometer scale is of great interest for the incorporation of bioactive

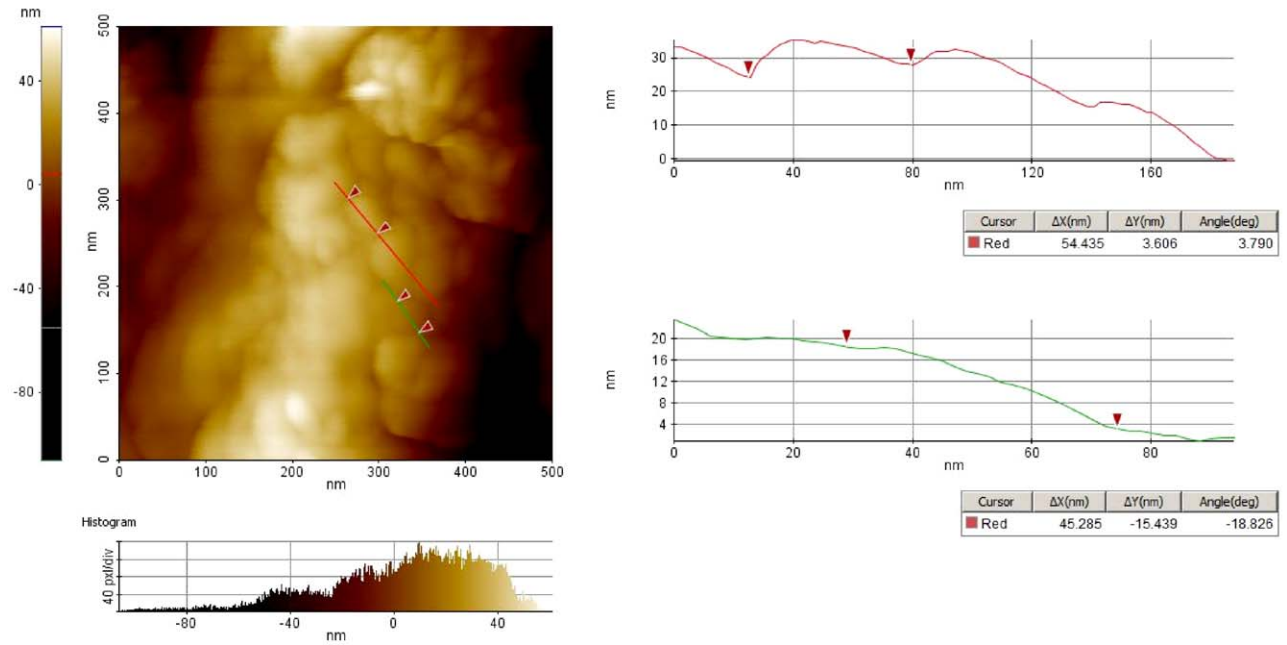

FIGURE 3. AFM image of BGNPF and particle size analysis.

glasses in oral hygiene products, as they are more regular, less abrasive and devoid of sharp edges, thus less harmful to gingival tissue and mucous membranes. These features are a great advantage for their use in procedures for HD treatments, especially in cases that involve brushing and friction in the region of operation.

Figure 4 shows the DRX spectra for FBGMP and FBGNP, both with 9.28% CaF_2 and treated at 700°C, and the diffraction patterns of CaF_2 and $Ca(NO_3)_2$. It can be seen that the FBGNP sample presented main crystalline peaks at approximate values 29, 34 and 46°, allocated to both HA and FAP. XRD patterns of FAP and HA overlap, and therefore, it is not possible to distinguish between these two phases based only on this technique.[9] The presence of these phases can be explained, according to Oliveira,[15] based on two different events. Initially, the aqueous environment in the sol–gel process may generate precipitation of HA and, hence, in this study also fluorapatite, due to the presence of fluoride during the synthesis procedure. A second hypothesis is that the temperature used for the heat treatment was sufficient to increase the mobility of Si, Ca and P ions in the glass structure, resulting in the crystallization of the material. This hypothesis is especially applied to the system analyzed in the present study, since crystallization begins at the surface and the nanoparticles have a high surface area (Hong et al., 2009). XRD pattern of FBGMP showed a band between 15° and 40° related to amorphous silica, and peaks similar to those of CaF_2. It is possible to assume that other peaks related to apatite and fluorapatite in this sample may be overlapped by the amorphous silica band.[9] This hypothesis will be discussed later, along with the XPS analysis.

Figure 5 shows the Nitrogen adsorption/desorption isotherms for BGNPF. BET analysis showed that nanoscale affects the pore structure and surface area. Surface area and pore volume, obtained by BET, were 10.2 $m^2\ g^{-1}$ and 0.02 $cm^3\ g^{-1}$, respectively.

Results reported in Table I show that the BGNPF presented lower surface area and lower pore volume, compared to BGMPF. These two materials were obtained by different synthetic techniques. As BGMPF were synthesized by the traditional sol–gel technique an aerogel was obtained, which are mesoporous materials with high surface area. Ultrasound was used only for mixing the components of the precursor solution of BGMPF. The lower surface area obtained for the nanoparticles can be explained by the fact that ultrasound was used throughout the synthesis of BGNPF. Thus, the characteristics of sonogeis, such as higher density and homogeneous structure, are present in BGNPF, resulting in a lower surface area.[15]

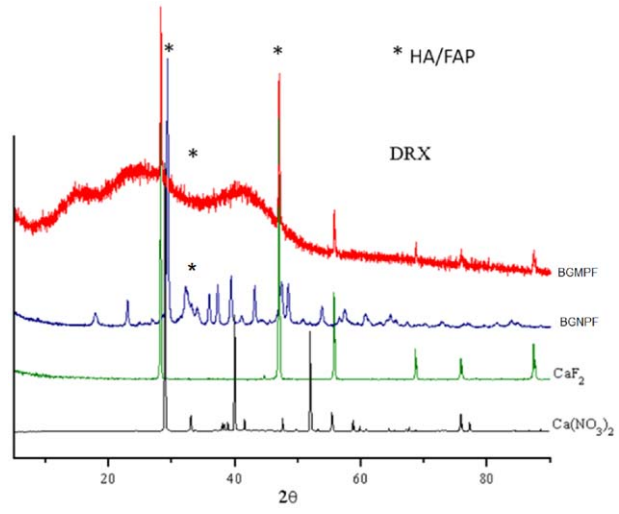

FIGURE 4. DRX spectra of BGMPF and BGNPF with 9.28% fluorine.

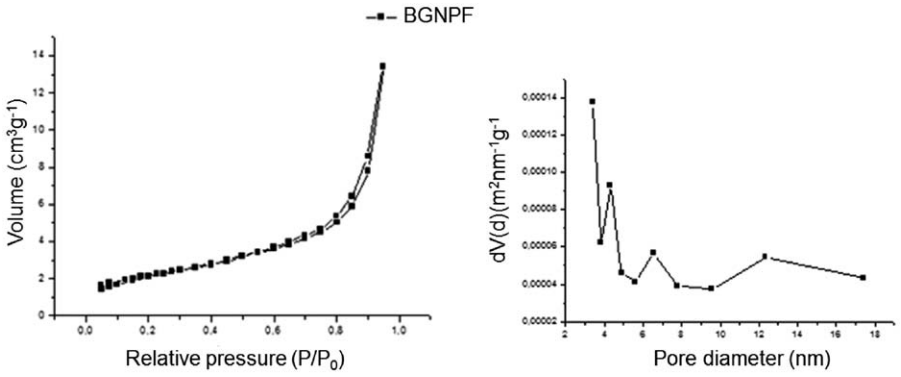

FIGURE 5. Nitrogen adsorption/desorption Isotherms and BJH analysis for BGNPF.

Table II shows surface elemental composition determinate by XPS for the bioactive glass nanoparticle sample containing 9.28% CaF_2 (BGNPF) and bioactive glass microparticles containing 9.28% CaF_2 (BGMPF) with and without the use of ultrasound during synthesis. Results indicate that C, Ca, O, P, and Si are mainly present on the surface of samples, In case of the sample BGNPF, was detected on the surface a considerable lower concentration of F in comparison with the samples BGMPF, suggesting that F is less exposed in the nanoparticles system in spite of this present a larger superficial area. The important amount of F on the surface of macro particles treated with ultrasound suggest that ultrasound effect favor to a different surface arrangement rich in F. Presence of N and C on samples surface possible is due to residual from the synthesis.

Figure 6 shows high-resolution XPS spectra of the F 1s region for the samples BGNPF and BGMPF with and without the use of ultrasound during synthesis.

It is possible to observe on the spectrum of the sample BGNPF an undefined and low intensity peak due the poor presence of F on the surface. However, the spectrum of the F1s obtained for the sample BGNPF without using ultrasound shows a peak with binding energy at 684,0 eV which is approximated to that one reported for F in FAP (684.2 eV) according with the literature.[16] A defined and more intense peak is observed in the spectrum obtained for the macro particles prepared using ultrasound. A fitting curve under the asymmetric signal allowed determinate two peaks that suggest the presence of two kinds of F on the sample surface. One at 684.0 eV corresponding to F in FAP and other majority at 686.4 eV that correspond to CaF_2.[16]

In a previous study a fluorapatite coating was evaluated using the XPS technique,[16] it was reported that existed only a signal of F1s attributed to F in FAP (at 684.2 eV), and no trace of F on CaF_2 (in 686,7 eV) concluding therefore, that the CaF_2 phase was not present. Comparing these results with those obtained in this study, shown in Figure 6, it can be assumed that CaF_2 reprecipitate only in BGMPF samples synthetized with ultrasound, and fluorapatite crystals are formed in BGMPF samples synthetized without ultrasound and in the BGNPF. These results are in accordance with the results found in the XRD analysis for FBGNP, which showed crystalline peaks related to hydroxyapatite and fluorapatite.

The results obtained by the XPS analysis allow us to affirm that the crystalline peaks showed in XRD analysis, initially assigned to both HA and FAP due to the overlap of the XRD patterns, are infact related to FAP, confirming the presence of this phase in the nanoparticles structure. However, it does not rule out the presence of HA phase in addition to FAP. This result is very important for the purpose of this study, which is to use this material in the dental field, where the presence of FAP is desirable.

These results are also consistent with those obtained by authors who have synthesized bioactive glass microparticles containing fluoride by the casting route. Lusvardi[12] showed the crystallization of the apatite phase in a bioactive glass containing fluoride and it appears to depend on upon the phosphate content in the glass. For low phosphate content in bioactive glass-containing fluoride, FAP does not form upon heat treatment.

Brauer[8] characterized the glass structure and the crystallization behavior in order to develop bioactive glasses, which crystallize FAP. Upon heat treatment, the glasses were crystallized with a mixture of sodium orthophosphate and calcium fluoride (compositions containing sodium) and fluorapatite (sodium-free composition). The fluoride suppressed spontaneous crystallization, allowing the formation of a glass–ceramic by controlled crystallization. A notable feature

TABLE I. Surface Area and Pore Volume of BGNPF and BGMPF

	BGMPF 9.28%	BGNPF 9.28%
Surface area	73.148 $m^2\ g^{-1}$	10.215 $m^2\ g^{-1}$
Pore volume	0.148 $cm^3\ g^{-1}$	0.022 $cm^3\ g^{-1}$

TABLE II. Surface Elemental Composition (At. %)

	Surface elemental composition (At. %)						
	O 1s	Ca 2p	C 1s	F 1s	P 2p	Si 2p	N 1s
BGNPF	51.6	19.8	21.7	0.5	2.2	4.3	ND
BGMPF with US	49.3	8.1	12.6	6.9	2.5	17.8	2.8
BGMPF without US	54.6	12.6	11.9	1.1	3.9	3.2	12.7

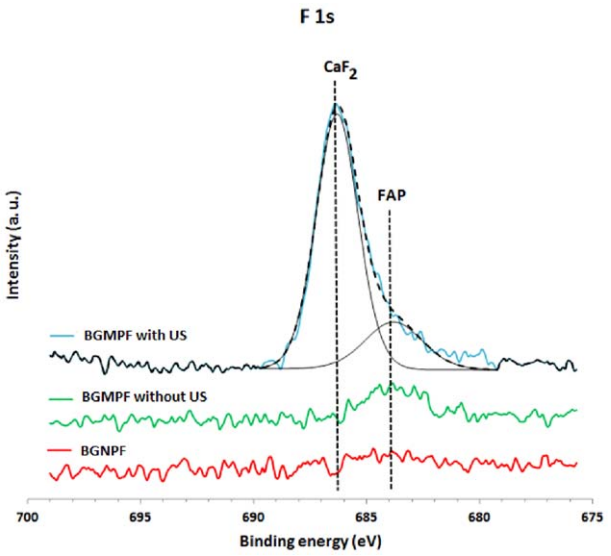

FIGURE 6. XPS spectra of BGNPF and BGMPF produced, in the region associated with fluoride.

is that the polymerization of the silicate network, and the network connectivity, are not changed during the crystallization, resulting in embedded orthophosphate and fluorapatite crystals within a matrix of bioactive glass. Therefore, it was concluded that if maintaining the high phosphate content and low sodium content, the glass–ceramic containing fluorapatite can be obtained, without affecting the structure of the bioactive glass silicate phase.

Considering the results obtained by both XRD and XPS analysis, and considering also the results reported in the literature, it is suggested that the formation of embedded fluorapatite crystals within the bioglass matrix occurred when the synthesis was performed by sol–gel route with ultrasound assistance, to produce nanoparticles and microparticles containing fluoride.

The developed system is of great importance for dentistry, since bioactive glasses are already used clinically as bone grafts. Additionally, this material present great interest to be used as implant coatings, dentifrices, and in all these applications the addition of fluoride would be beneficial. Fluoride is well known to prevent dental caries inhibiting demineralization of enamel and dentin, increasing remineralization and inhibiting bacterial enzymes. Glass ceramics containing FAP as crystalline phase is of great attention for dental and orthopedic applications, due to its better osseointegration and osteoconduction. If FAP crystals are embedded in a bioactive glass matrix material, they have the potential to combine the benefits of the osteoconductive crystalline phase of FAP with the bone-regenerative properties of the bioactive glass phase (1Chiau, 2012).

CONCLUSIONS

Fluorine-containing bioactive glass nanoparticles with a spherical shape were obtained by sol–gel method assisted by ultrasound energy. Evaluation of the particle size obtained by DLS (5.3 ± 0.3 nm) and by AFM (between 45 and 55 nm) showed a significant increase in particle size after heat treatment, suggesting agglomeration or aggregation. Considering the results obtained by both XRD and XPS analysis, it is suggested that the formation of embedded fluorapatite crystals within the bioglass matrix occurred when the synthesis was performed by sol-gel route with ultrasound assistance, to produce nanoparticles containing fluoride. The use of nanoscale bioactive glass containing fluoride, with high specific surface area and pore volume, favors the ability of this material to be deposited within the dentinal tubules. Thus, it is possible to conclude that this new system containing FBGNP is a potential material to improve the treatment of dentin hypersensitivity.

ACKNOWLEDGMENTS

The authors gratefully acknowledge the technical support on TEM/SEM analysis from the Center for Microscopy-UFMG/Brazil.

REFERENCES

1. Shiau HJ. Dentin hypersensitivity. J Evid Base Dent Pract 2012;12: 220–228.
2. Trushkowsky RD, Oquendo A. Treatment of Dentin Hypersensitivity. Dent Clin N Am 2011;55:599–608.
3. Tonetto MR, Dantas AAR, Bortolini GF. Dentin hypersensitivity: in search of an effective treatment. Rev Odontol 2012;24:190–199.
4. Chu CH, Lo ECM. Dentin hypersensitivity: a review. Hong Kong Dent J 2010;7:15–22.
5. Kokubo T. Bioceramics and their clinical applications, Boca Raton: CRC Press; 2008.
6. Labbaf S, Tsigkou O, Müller KH, Stevens MM, Porter AE, Jones JR. Spherical bioactive glass particles and their interaction with human mesenchymal stem cells *in vitro*. Biomater 2011;32:1010–1018.
7. Pritsos C, Kontonasaki E, Chatzistavrou X, Papadopoulou L, Pappas F, Koidis P, Paraskevopoulos KM. Studying morphological characteristics of thermally treated bioactive glass using image analysis. J Eur Ceram Soc 2005;425:891–897.
8. Brauer DS, Anjum MN, Mneimne M, Wilson RM, Doweidar H, Hill RG. Fluoride-containing bioactive glass-ceramics. J Non-Cryst 2012;358:1438–1442.
9. Brauer DS, Karpukhin N, O'Donnell MD, Law RV, Hill RG. Fluoride-containing bioactive glasses: Effect of glass design and structure on degradation, pH and apatite formation in simulated body fluid. Acta Biomater 2010;6:3275–3282.
10. Brauer DS, Al-Noaman A, Hill RG, Doweidar H. Densitystructure correlations in fluoride-containing bioactive glasses. Mater Chem Phys 2011;130:121–125.
11. Gentleman E, Stevens MM, Hill RG, Brauer DS. Surface properties and ion release from fluoride-containing bioactive glasses promote osteoblast differentiation and mineralization *in vitro*. Acta Biomater 2013;9:5771–5779.
12. Lusvardi G, Malavasi G, Menabue L, Aina V, Morterra C. Fluoride-containing bioactive glasses: Surface reactivity in simulated body fluids solutions. Acta Biomater 2009;5:3548–3562.
13. Reed JS. Principles of Ceramic Processing. New York: Wiley; 1994.
14. Lynch E, Brauer D, Karpukhina N, Gillam DG, Hill RG. Multi-component bioactive glasses of varying fluoride content for treating dentin hypersensitivity. Dent Mater 2011;28:168–178.
15. Oliveira AAR, Carvalho SM, Mansur HS, Pereira MM. Synthesis and Characterization of Bioactive Glass Particles using an Ultrasoundassisted Sol-Gel process: Engineering the Morphology and Size of Sonogels via a Poly(ethylene glycol) Dispersing Agent. Mater Lett 2014;33:44–48.
16. Cheng K, Zhang S, Weng W. Surf Coat Tech 2005;198:237–241.
17. Tirapelli C, Panzeri H, Soares RG, Peitl O, Zanotto ED. A novel bioactive glass-ceramic for treating dentin hypersensitivity. Braz Oral Res 2010;24:381–387.
18. Hong Z, Reis RL, Mano JF. reparation and in vitro characterization of novel bioactive glass ceramic nanoparticles. J Biomed Mater Res A 2009;88A:304–313.